

Supporting information

Polyrotaxane-like metal-organic framework showing luminescent sensing of Eu^{3+} cation and proton conductivity

**Bai-Qiao Song, Xin-Long Wang,* Guang-Sheng Yang, Hai-Ning Wang, Jun Liang,
Kui-Zhan Shao and Zhong-Min Su***

Institute of Functional Material Chemistry; Key Laboratory of Polyoxometalate
Science of Ministry of Education, Northeast Normal University, Changchun, 130024
Jilin, People's Republic of China ; E-mail: wangxl824@nenu.edu.cn,
zmsu@nenu.edu.cn

Table S1. Selected bond lengths (Å) and bond angles (°)

Bond lengths (Å)			
Cd(1)-O(4)	2.246(3)	Cd(1)-O(12)#1	2.558(3)
Cd(1)-O(13)#1	2.270(3)	Cd(2)-O(15)#2	2.303(3)
Cd(1)-O(5)	2.387(3)	Cd(2)-O(7)	2.359(3)
Cd(1)-O(6)	2.415(3)	Cd(2)-O(8)	2.171(3)
Cd(1)-O(1)	2.419(4)	Cd(2)-O(11)#2	2.428(3)
Cd(1)-O(14)	2.541(3)		

Bond angles (°)			
O(4)-Cd(1)-O(13)#3	133.19(13)	O(1)-Cd(1)-O(14)	80.16(15)
O(4)-Cd(1)-O(5)	96.31(13)	O(6)-Cd(1)-O(14)	86.00(11)
O(13)#3-Cd(1)-O(5)	92.56(14)	O(4)-Cd(1)-O(12)#3	80.49(11)
O(4)-Cd(1)-O(1)	115.14(15)	O(13)#3-Cd(1)-O(12)#3	53.29(12)
O(13)#3-Cd(1)-O(1)	90.43(15)	O(5)-Cd(1)-O(12)#3	91.83(12)
O(5)-Cd(1)-O(1)	132.66(13)	O(1)-Cd(1)-O(12)#3	126.13(14)
O(4)-Cd(1)-O(6)	130.68(11)	O(6)-Cd(1)-O(12)#3	131.62(11)
O(13)#3-Cd(1)-O(6)	90.95(12)	O(14)-Cd(1)-O(12)#3	134.17(11)
O(5)-Cd(1)-O(6)	54.33(10)	O(8)-Cd(2)-O(7)	80.88(14)
O(1)-Cd(1)-O(6)	78.40(13)	O(15)#4-Cd(2)-O(7)	85.42(13)
O(4)-Cd(1)-O(14)	53.68(12)	O(8)-Cd(2)-O(11)#4	105.03(14)
O(13)#3-Cd(1)-O(14)	170.51(14)	O(15)#4-Cd(2)-O(11)#4	55.56(13)
O(5)-Cd(1)-O(14)	92.95(15)	O(7)-Cd(2)-O(11)#4	138.37(13)

Symmetry transformations used to generate equivalent atoms: #1= $x, -y+2, z-1/2$;
#2 = $x, -y-1, z-1/2$; #3 = $x, -y+2, z+1/2$; #4= $x, -y-1, z+1/2$;

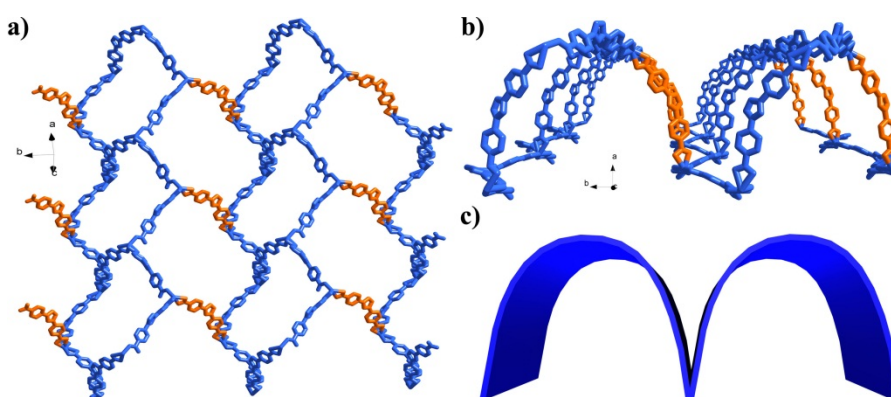


Fig. S1 a) and b) The loop-like chains are bridged by L^- to form a 2D infinite bow-shaped (6,3) layer. C) schematic representation of the 2D infinite bow-shaped (6,3) layer.

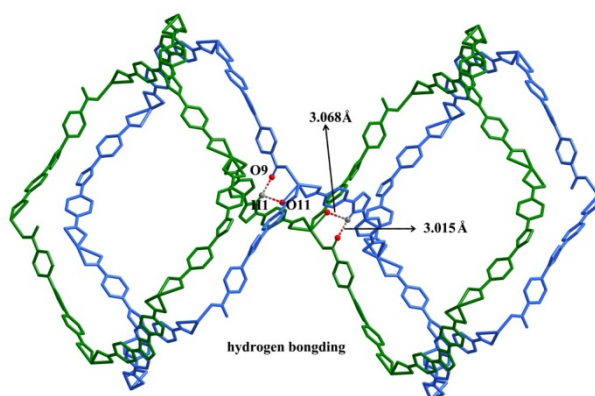


Fig. S2 The strong hydrogen bonding ($\text{C-H}\cdots\text{O} = 3.015\text{-}3.068 \text{ \AA}$) between the oxygen atoms belong to the $[\text{Cd}_6\text{L}_6]$ 6-membered ring from one 3-fold interpenetration network and the highly acidic methylene hydrogen of the imidazolium moiety of the ligand rod from another 3-fold interpenetration network.

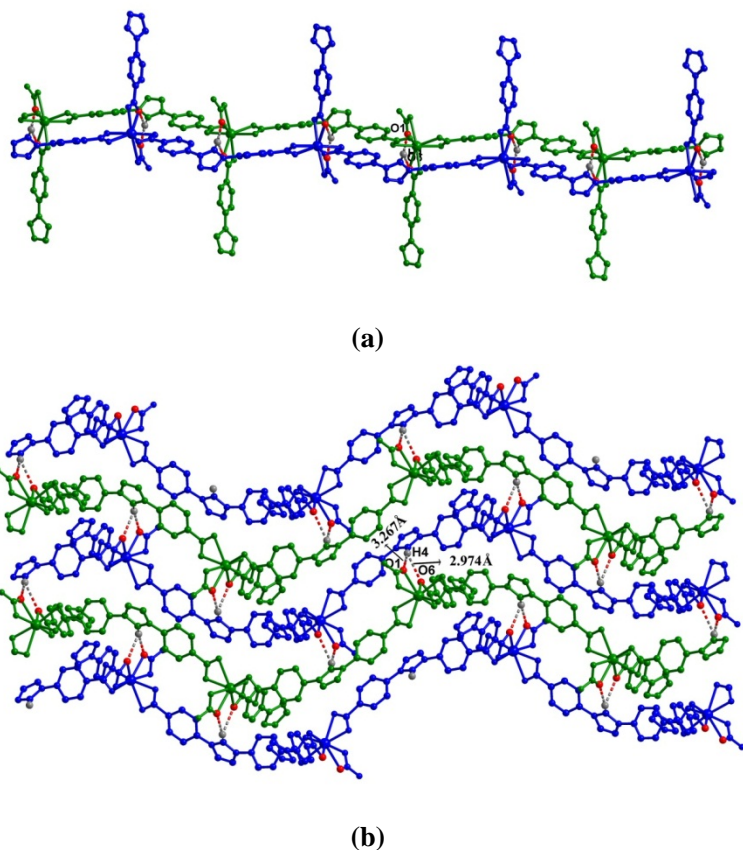


Fig. S3 (a) The interdigitated model in **1**. (b) The strong hydrogen bonding ($\text{C-H}\cdots\text{O} = 2.345\text{-}2.630 \text{ \AA}$) in the interdigitated model in **1**.

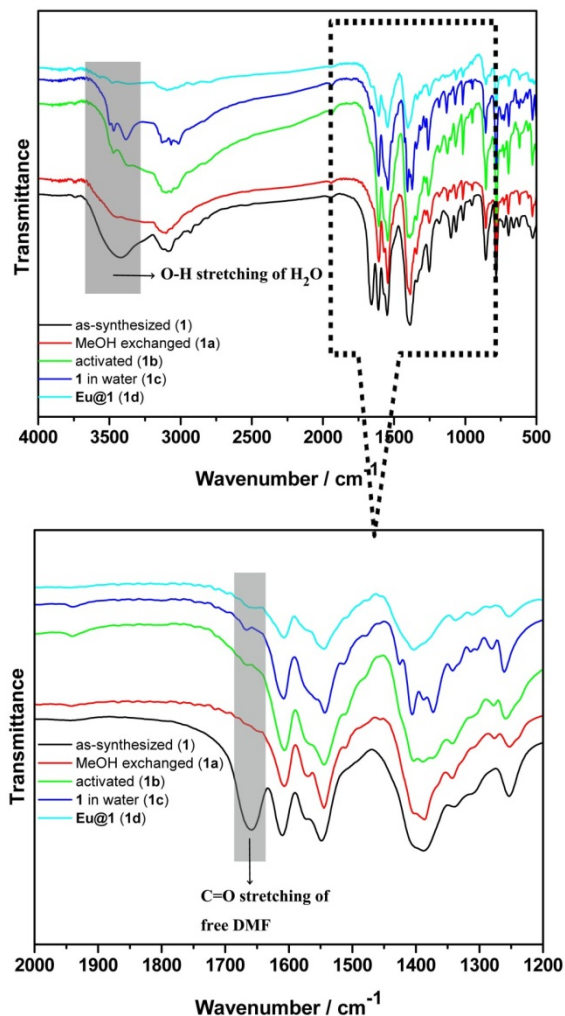


Fig. S4 Infrared spectrum of fresh **1**, MeOH-exchanged (**1a**), activated (**1b**), **1** in water (**1c**), and **Eu@1** (**1d**). The broad peak at 3421 cm⁻¹ in the IR spectrum of **1** indicates the presence of water molecules in the structure. Sharp peaks at 1658 and 1610 cm⁻¹ ascribe to CO stretching vibrations of the free and coordinated dimethylformamide molecules, respectively, inside the channels. Another sharp peak at 1388 cm⁻¹ appears due to the presence of coordinated nitrate anions. The complete removal of the free DMF and H₂O molecules was verified by the disappearance of the vibration at 1658 cm⁻¹ and 3421 cm⁻¹ in **1a** and **1b**, respectively. Interestingly, when fresh samples of **1** were immersed in 0.3 mol / L DMF solution of Eu(NO₃)₃ for 5 days to get **Eu@1**, the IR spectrum of **Eu@1** shows scarcely any free DMF and H₂O molecules in it.

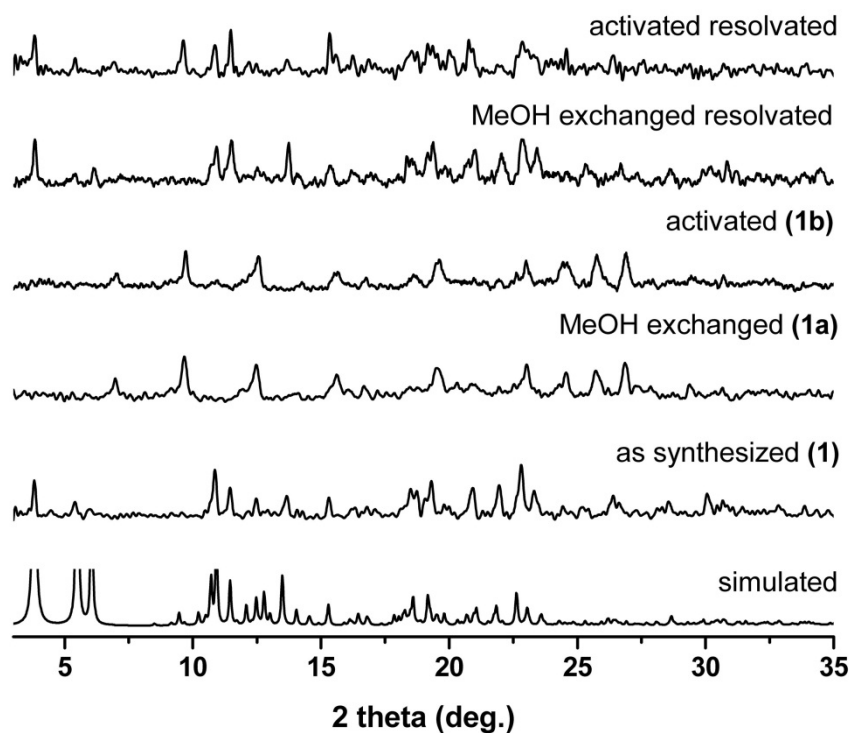


Fig. S5 PXR profiles of as-synthesized (**1**), MeOH-exchanged (**1a**), activated (**1b**), and resolvated samples.

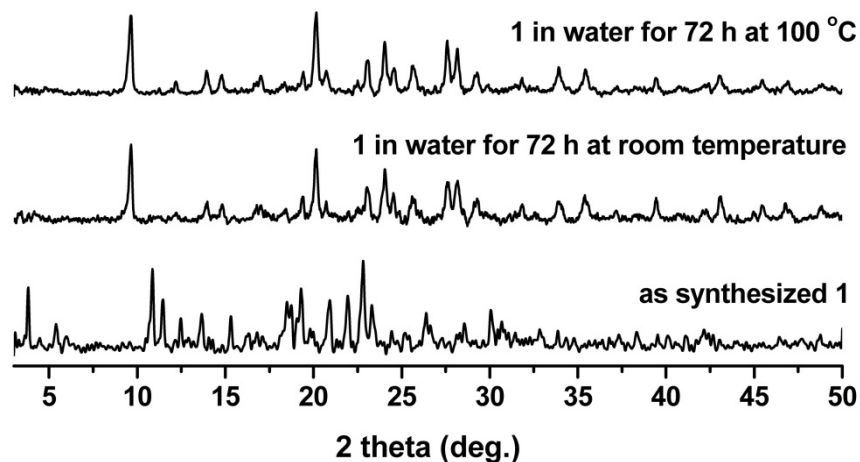


Fig. S6 PXR profiles of as-synthesized samples and the as-synthesized samples in water under different conditions.

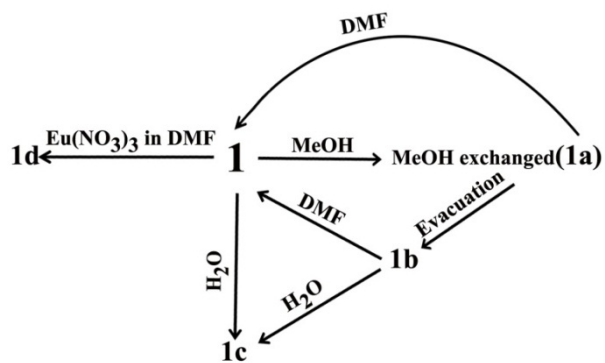
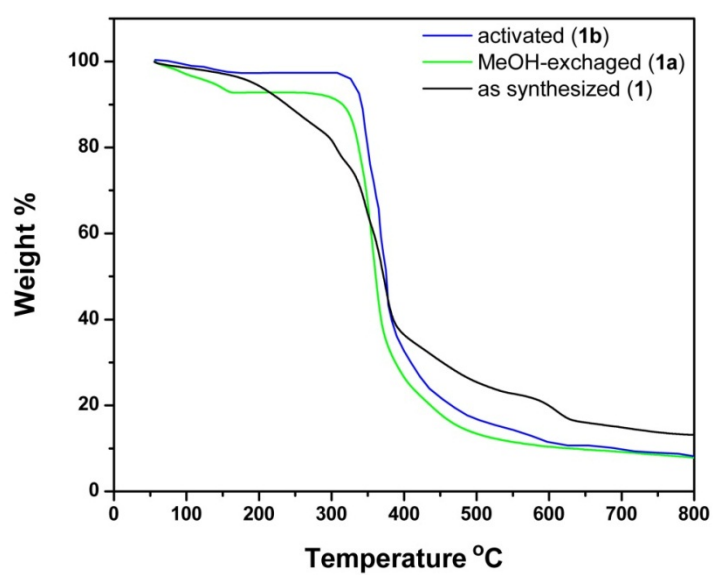
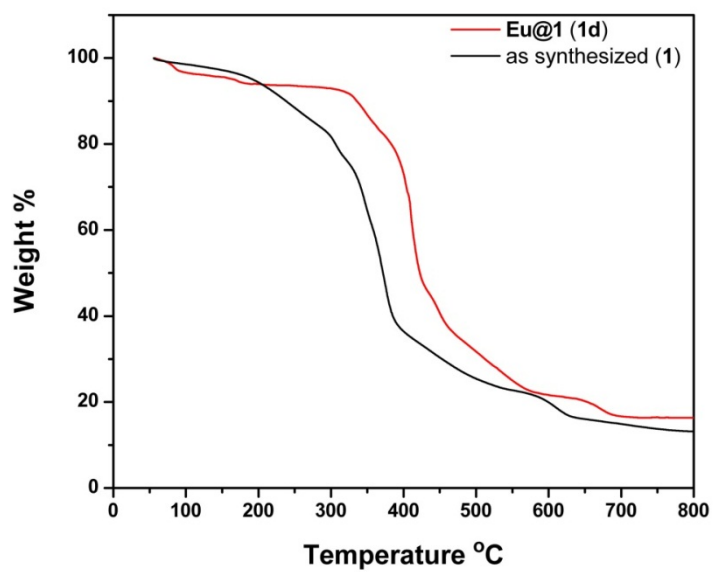


Fig. S7 The phase transformation during different process.



(a)



(b)

Fig. S8 (a) TGA curves of compound **1**, MeOH-exchanged samples (**1a**), and activated samples of **1b**. (b) TGA curves of compound **1** and samples of **Eu@1 (1d)**.

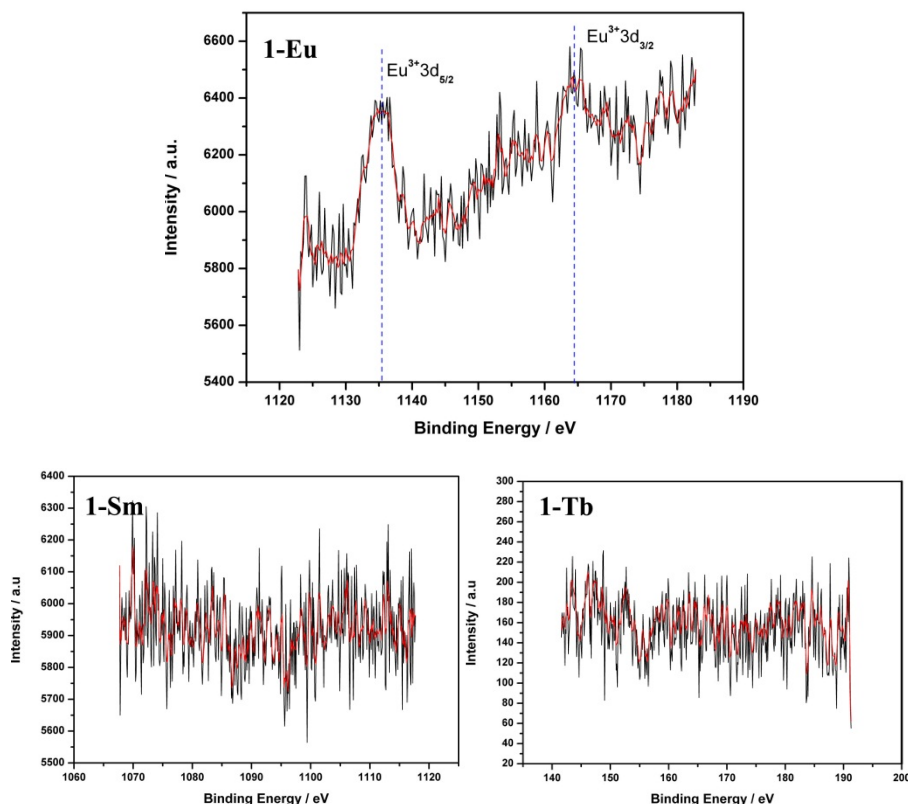


Fig. S9 Eu 3d, Sm 3d, Tb 4d XPS spectra for **1-Eu**, **1-Sm**, **1-Tb**, respectively. **1-Ln³⁺** represents the samples which were immersed in 0.3 mol / L DMF solution of nitrate salts of Ln³⁺ cations for 5 days. In the XPS spectrum of **1-Eu**, the peaks at 1135.2 eV and 1165.1 eV are assigned to the Eu 3d_{5/2} and Eu 3d_{3/2}, respectively. But for **1-Sm** and **1-Tb**, no peaks for Sm 3d and Tb 4d are found.

Table S2. ICP analysis for the samples which were immersed in 0.3 mol / L DMF solution of nitrate salts of Ln³⁺ cations for 5 days

ICP	1-Eu	1-Tb	1-Sm	1-Dy
Cd	19.81%	20.97%	20.95%	21.00%
Ln	2.95%	0	0	0
Ln:Cd(wt:wt)	0.15:1	0	0	0
Ln:Cd(molar:molar)	0.11:1	0	0	0

1-Ln³⁺ represents the samples which were immersed in 0.3 mol / L DMF solution of nitrate salts of Ln³⁺ cations for 5 days.

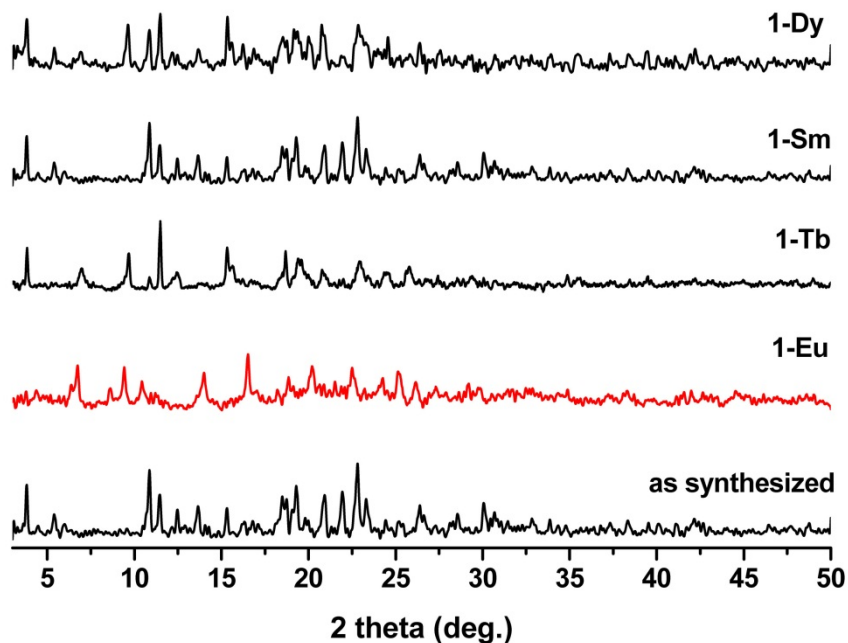


Fig. S10 PXRD profiles of as-synthesized samples and **1-Ln** samples which were soaked in 0.3 mol / L DMF solution of nitrate salts of Ln^{3+} cations for 5 days.

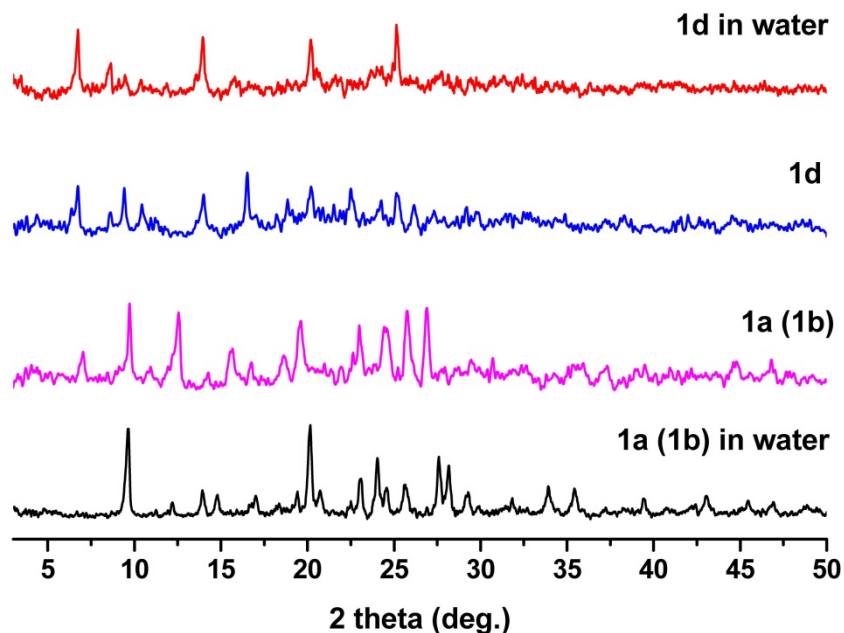
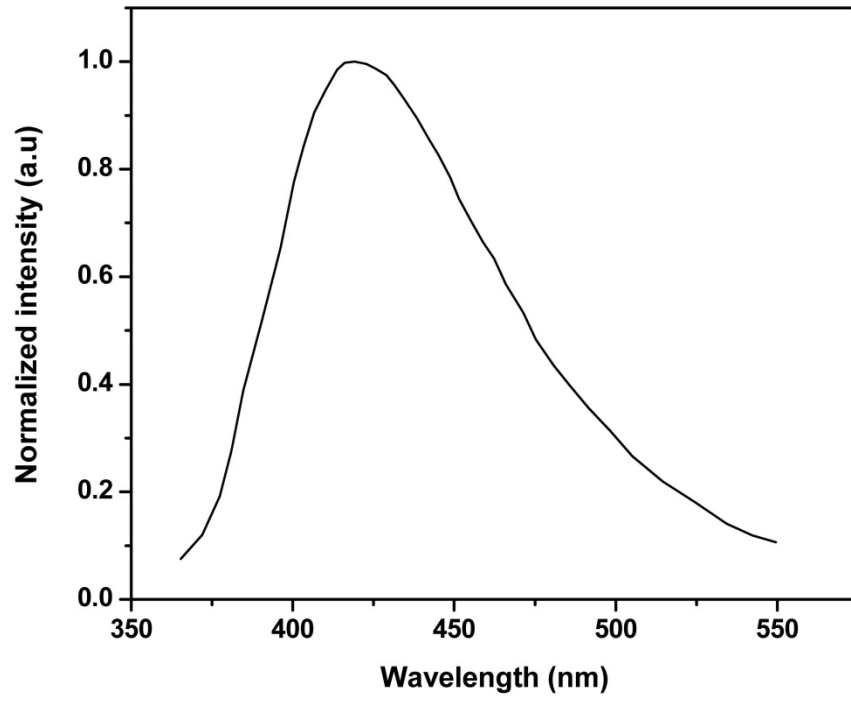
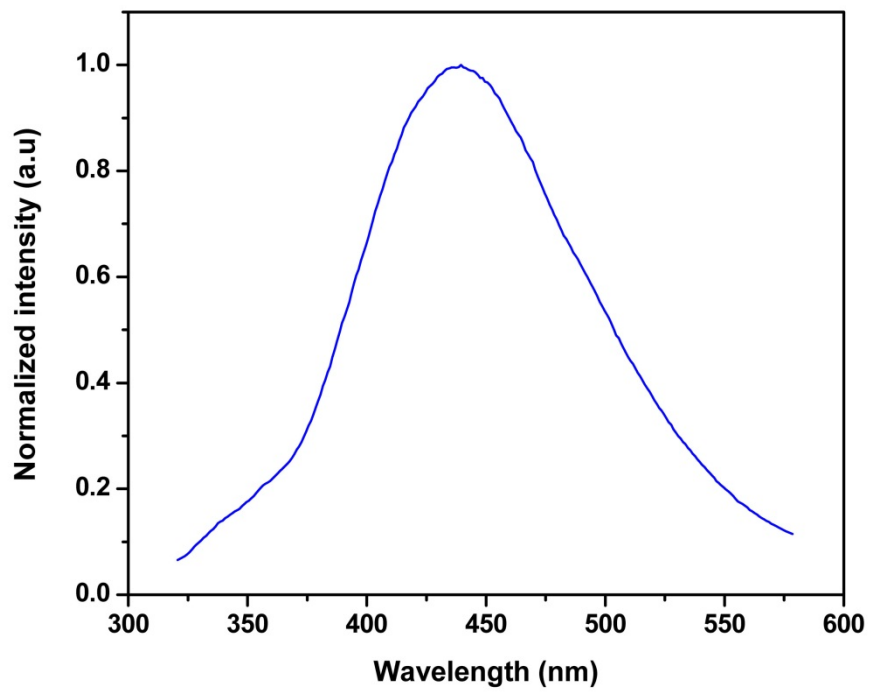


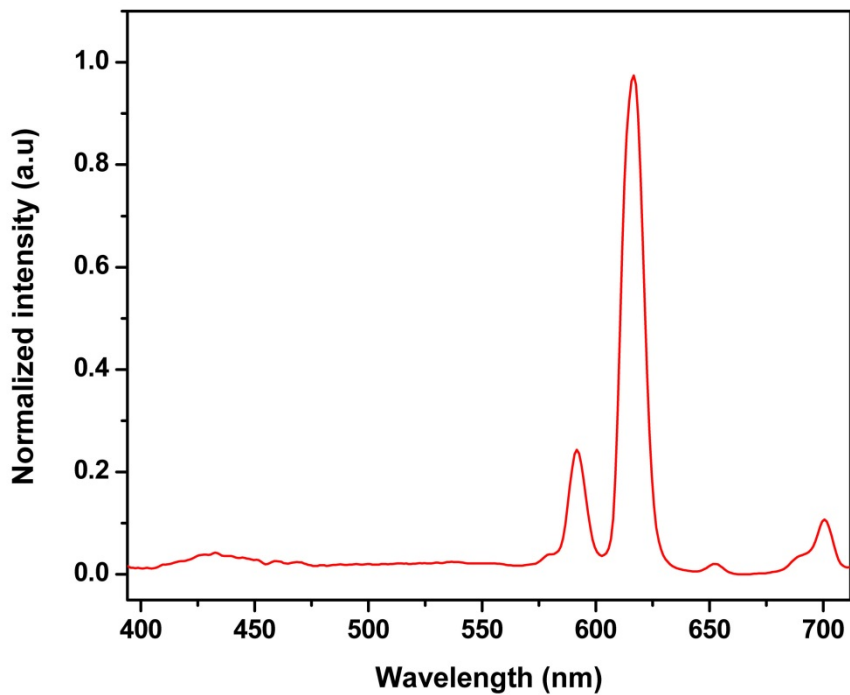
Fig. S11 PXRD profiles of MeOH-exchanged (**1a**) samples, desolvated samples (**1b**), samples of **1a** or **1b** in water, samples of **Eu@1** (**1d**), and samples of **1d** in water.



(a)

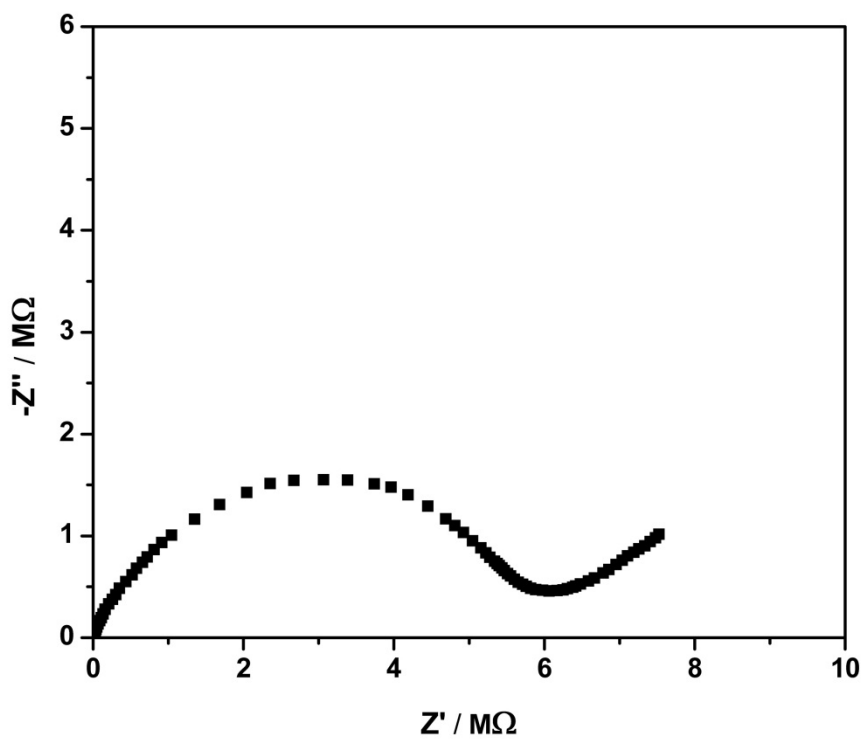


(b)

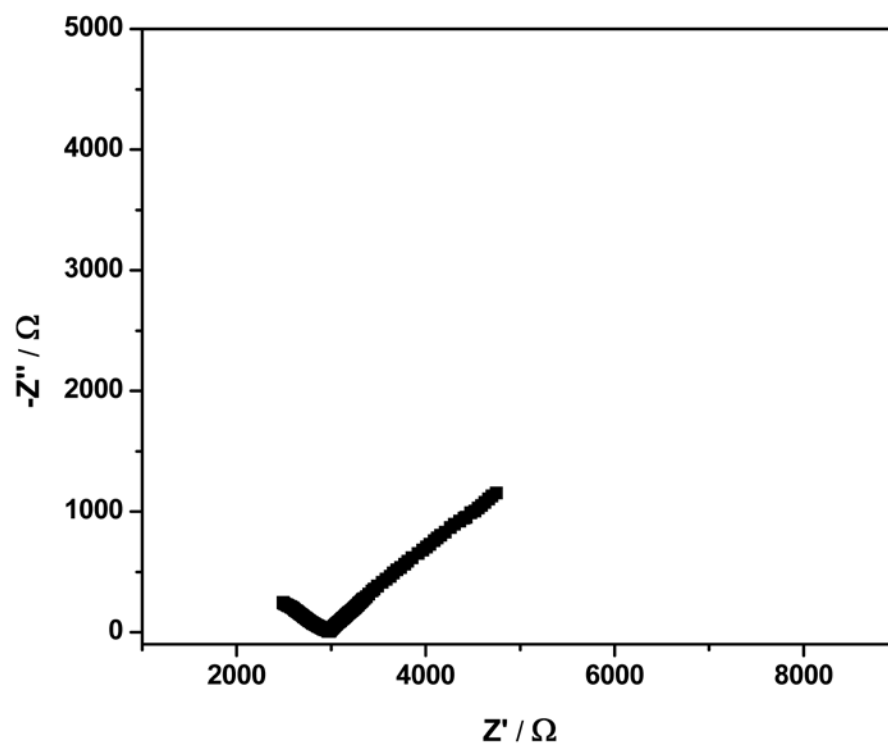


(c)

Fig. S12 (a) Solid-state photoluminescent spectra of $\text{H}_2\text{L}^+\text{Cl}^-$ ($\lambda_{\text{ex}} = 340$ nm and $\lambda_{\text{em}} = 420$ nm). (b) Solid-state photoluminescent spectra of **1** ($\lambda_{\text{ex}} = 340$ nm and $\lambda_{\text{em}} = 438$ nm). (c) The visible emission spectra of **Eu@1** with $\lambda_{\text{ex}} = 340$ nm in DMF.



(a)



(b)

Fig. S13 Some of the Nyquist plots for **1** at 298 K under different relative humidity (a) 40 % (b) 98 %.